

RAIN EFFECTS ON ASCAT RETRIEVED WINDS

Wenming Lin¹, Marcos Portabella², Ad Stoffelen³, Antonio Turiel¹, Anton Verhoef³, Jeroen Verspeek³,
Joaquim Ballabrera², Jur Vogelzang³

¹Institut de Ciències del Mar (ICM-CSIC), Barcelona, Spain

²Unitat de Tecnologia Marina (UTM-CSIC), Barcelona, Spain

³Royal Netherlands Meteorological Institute (KNMI), De Bilt, The Netherlands

Email: wenminglin@cmima.csic.es

ABSTRACT

In this study, the rain impact on the ASCAT operational Level 2 retrieved wind quality and the effectiveness of the quality control (QC) are investigated. It is shown that ASCAT is much less affected by direct rain effects, such as ocean splashing, but effects of increased wind variability appear to dominate. The operational QC proves to be effective in screening these artifacts, but at the expense of valuable winds. An image processing method, known as the singularity analysis, is proposed in this study to complement the current QC, and its potential is illustrated.

Index Terms— ASCAT, rain effects, quality control, MLE, singularity analysis

1. INTRODUCTION

The Advanced Scatterometer (ASCAT) is one of the instruments onboard the Metop-A satellite, which was launched on 19 October, 2006. It is a real aperture, C band, vertically polarized radar with three fan beam antennas pointing to the left hand side of the sub-satellite track and three fan beam antennas pointing to the right hand side [1]. Scatterometers are known to provide accurate mesoscale (25-50 km resolution) sea surface wind field information used in a wide variety of applications, including Numerical Weather Prediction (NWP) data assimilation, nowcasting, ocean forcing and climate studies. However, scatterometers are sensitive to geophysical phenomena other than wind vector cell (WVC) mean wind, such as rain, local wind variability, confused sea state, and the radar footprint contamination by land or ice. These phenomena can distort the WVC-mean wind signal, leading to poor-quality retrieved winds. As such, recognition, and then correction or elimination of poor-quality data is a prerequisite for the successful use of scatterometer winds.

Rain is known to both attenuate and scatter the microwave signal [2] in the atmosphere. As the rain rate increases, the radar receives less of the radiation scattered by the surface, and more of the radiation scattered by the rainy layer that becomes optically thicker due to volumetric

Rayleigh scattering [3]. The lower the wavelength of the radar signal, the larger is the impact of both effects (rain attenuation and scattering). In addition to these effects, there is a “splashing” effect. The roughness of the sea surface is increased because of splashing due to rain drops. This increases the radar backscatter (σ^0) measured, which in turn will affect the quality of wind speed (positive bias due to σ^0 increase) and direction (loss of anisotropy in the backscatter signal) retrievals. In case of moderate or high winds, where ocean roughness is dominated by wave breaking, the splash effect becomes small.

Another effect associated with heavy rain is increased wind variability. Convective rain cools the air underneath the rain cloud which reinforces downdraft near convective cells. These downdrafts often hit the ocean surface and cause outflow over the ocean, leading to variable wind speeds and directions. Such variability within a WVC would increase the isotropy of the radar backscattering at the ocean surface, yielding lower quality wind retrievals.

In this paper, the rain impact on ASCAT-derived winds as well as the effectiveness of the current operational QC are assessed. In addition, a new QC technique, based on an image processing method, i.e., the singularity analysis, is proposed and tested. For such purpose, ASCAT winds are collocated with the European Centre for Medium-range Weather Forecasts (ECMWF) winds, the Tropical Rainfall Measuring Mission’s (TRMM) Microwave Imager (TMI) rain data, and the tropical moored buoy wind and precipitation data. Section 2 introduces the current approach of ASCAT QC, as well as the concept of singularity analysis. Section 3 presents a few results based on the analysis of the collocated data set. Finally, the conclusions can be found in section 4.

2. METHODOLOGY

Several methodologies have been proposed over the last 10-15 years to address the rain issue in scatterometry, notably for Ku-band systems [4], [5], [6]. For the operational Level 2 ASCAT Wind Data Processor (AWDP), developed in the framework of the European Organization for the Exploitation of Meteorological Satellites (EUMETSAT)

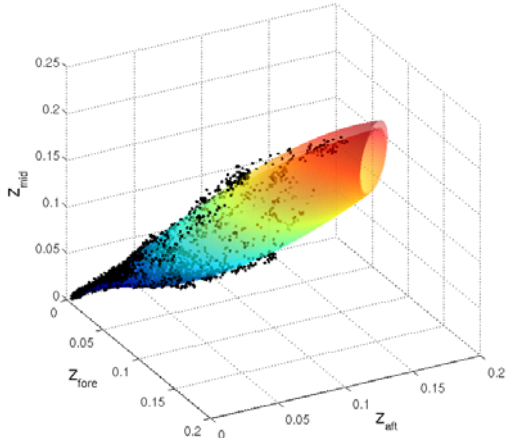


Fig. 1. Visualization of the CMOD5n GMF (color surface) and the ASCAT-measured triplets (black dots) for WVC number 21. The axes represent the fore-, aft- and mid-beam backscatter measurements in Z-space, where $z = (\sigma^0)^{0.625}$.

Numerical Weather Prediction (NWP) Satellite Application Facility (SAF), a quality control has been developed. This QC is based on the inversion residual or Maximum Likelihood Estimator (MLE) information [7], which can be interpreted as the closest distance of the ASCAT backscatter measurement set (namely ‘triplet’, corresponding to the three antenna beams in each side of the satellite swath) in a WVC, to a conical surface, which represents the Geophysical Model Function in the 3-D measurement space (see Fig. 1). Such cone as constructed from the so-called CMOD5n GMF [8], represents the best known fit to the measured triplets and can in turn be used for Quality Control (QC) purposes. For a given WVC position across the swath, the conical surface mostly depends on just two geophysical parameters, i.e., wind speed and direction.

In general, the triplets lie close to the cone surface, corresponding to low MLE values. As shown by several QC procedures developed for previous scatterometer missions [4], [7], [9] a large inconsistency with the GMF results in a large MLE, which indicates geophysical conditions other than those modeled by the wind GMF, such as rain, local wind variability, confused sea state, or ice. As such, the MLE provides a good indication for the quality of the retrieved winds. Recent work [10] shows that for triplets located outside the cone surface, the quality of the retrieved winds is good regardless of their distance to the cone surface, i.e., MLE value. To account for this different behavior inside and outside the cone surface, a sign is assigned to the MLE value, depending on whether the triplet is located inside (positive) or outside (negative) the cone surface. In the current version of the AWDP, any WVC with $MLE > +18.6$ is flagged as poor wind quality. Although the ASCAT QC has proved to be very effective in rejecting WVCs with poor wind quality while keeping those with good quality, it has not been specifically tested for rain effects until recently [10].

On the other hand, an image processing technique,

Table 1. VRMS difference between ASCAT and buoy winds and between ECMWF and buoy winds.

Category	Number	ASCAT-Buoy(m/s)	ECMWF-Buoy(m/s)
A (2h-RR<0.1, 1D-RR<0.1 mm/hr)	2650	1.57	2.16
B (2h-RR<0.1, 1D-RR≥0.1 mm/hr)	506	2.41	3.34
C (2h-RR≥0.1, 1D-RR≥0.1 mm/hr)	198	3.45	4.00

known as Singularity Analysis (SA), has been recently proposed as a complementary QC tool, in addition to the current ASCAT MLE-based QC. Singularity analysis is a welcome technique used to assess the presence of multifractal structure associated with turbulent flows. It has been successfully applied to derive the streamlines of ocean surface circulation from remote-sensing data of scalar variables [11]. It can also be used to detect acquisition and/or processing errors in remote-sensing maps, therefore opening the way to improve quality control procedures. Given a wavelet $\Psi(\mathbf{x})$, we define the wavelet transform of the gradient of a two-dimensional scalar signal s at the point \mathbf{x} and scale r , denoted by $T_{\Psi}|\nabla s|(\mathbf{x}, r)$, as [11] [12]

$$T_{\Psi}|\nabla s|(\mathbf{x}, r) = \int d\mathbf{y} |\nabla s|(\mathbf{y}) \frac{1}{r^2} \Psi\left(\frac{\mathbf{x}-\mathbf{y}}{r}\right) \quad (1)$$

where the wavelet projection depends on the scale resolution parameters as a power law, characterized by the local singularity exponents $h(\mathbf{x})$ in the way [11] [12],

$$T_{\Psi}|\nabla s|(\mathbf{x}, r) = \alpha(\mathbf{x}) r^{h(\mathbf{x})} + O(r^{h(\mathbf{x})}) \quad (2)$$

where the expression $O(r^{h(\mathbf{x})})$ means a term which is negligible compared to $r^{h(\mathbf{x})}$ when $r^{h(\mathbf{x})}$ goes to zero. The singularity exponent of a point is a dimensionless measure of the local regularity and the scaling properties of the scalar at that point. It is stable and scale invariant. Negative values of singularity exponents mean that the function is less regular, while positive values indicate a more regular behavior. Since the rainy areas usually correspond to a high deviation of the measured σ^0 from the empirical model, which in turn increases the inversion residual and decreases the retrieved wind quality, we are mostly interested in the irregular behaviors within the signal transformations carried out by SA.

3. MAIN RESULTS

Figure 2 shows the histogram of MLE values for different rain rate (RR) intervals. As shown by [10], there is a clear shift of the MLE distributions towards positive MLE values as RR increases. At TMI-RR= 0 mm/hr, the MLE distribution is almost symmetric with respect to the cone surface, corresponding to the same distribution of measurements inside and outside the cone. In contrast, at RR above 6 mm/hr, most of the WVC triplets are located inside the cone, with a substantial amount of triplets located very far away from the surface (large positive MLE values).

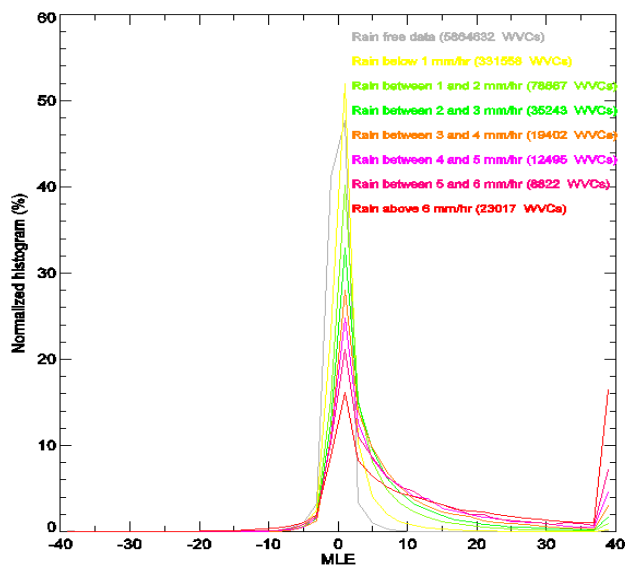


Fig. 2. MLE histogram for different rain rate (RR) intervals. Note that every colored line corresponds to a different RR interval (see legend). The number of WVCs for each histogram is also provided in the legend.

However, by using the operation QC threshold ($MLE > +18.6$), a substantial portion of the heavy-rain contaminated WVCs are not filtered out.

To better disentangle the ASCAT and ECMWF rain effects, an independent wind source, such as buoy wind information, is required. Two different RR parameters have been computed from buoy rain gauge time series: a 2-hourly RR and a daily average RR. The presence of significant 2-hourly RR should be a good indicator for rain contamination of the ASCAT backscatter signal. While the daily RR product is expected to effectively segregate rainy areas from dry areas, since atmospheric waves in the tropics are rather large-scale. A simple analysis using a combination of the two RR products and two different RR intervals, i.e., $RR < 0.1$ mm/hr and $RR > 0.1$ mm/hr, is carried out. Table 1 shows the Vector Root-Mean-Square (VRMS) difference between ASCAT and buoy winds (third column) and between ECMWF and buoy winds (fourth column) for categories A, B, and C. In general, ASCAT winds are in better agreement with buoy winds than those of ECMWF, indicating that ASCAT resolves smaller scales than ECMWF. In B, where the presence of rain-induced downdrafts is likely, ASCAT winds are clearly in better agreement with buoy winds than ECMWF. In C, the VRMS scores are higher than those in B. Although ASCAT is still in better agreement with buoys than ECMWF, the difference in VRMS is smaller. This suggests a possible influence of the rain splashing effect in the ASCAT retrieval quality. In summary, it turns out that ECMWF does not well resolve the air flow under rainy conditions. As such, one should be careful to draw conclusions when ECMWF wind is adopted as reference for assessing the rain impact on the ASCAT wind retrieval quality. Moreover, the air-sea interaction of

Table 2. VRMS difference between ASCAT and ECMWF winds for WVCs with singularity exponents (SE) < -0.2 and > -0.2 respectively. The statistic of QC-rejected WVCs is also presented for reference.

	SE > -0.2	SE < -0.2	QC-rejected
Number	1006	134	48
VRMS (m/s)	2.81	4.54	3.72

the ECMWF model in rainy conditions will be very different due to the lack of convective and dry downdrafts.

Figure 3 shows an ASCAT retrieved wind field with TMI collocated rain rate values superimposed. Figure 4 shows the corresponding singularity map. The map is constructed as the minimum exponents of the singularity maps associated to the zonal (U) and the meridional (V) wind components, which were independently processed as scalars. As shown in Figure 4, the presence of heavy rain bands induces clear singularity fronts as expected near downdraft boundaries, i.e., the places at which the value of singularity exponents is most negative. Also note that the values of singularity exponents all over the rain affected area are significantly smaller than those outside the rainy area, which is again in line with the erratic appearance of downdrafts in rainy areas. Table 2 presents the VRMS difference between ASCAT and ECMWF winds for WVCs with singularity exponents < -0.2 and > -0.2 respectively. It confirms that the most negative singularity exponents correspond to a high deviation of ASCAT winds from ECMWF winds. As already mentioned, this high deviation is likely caused by the lack of downbursts in the ECMWF model and, as such, more in depth analysis of the rain impact on ASCAT wind quality is required to optimize the ASCAT QC and wind retrieval near convection.

4. CONCLUSIONS

The MLE appears effective in screening effects of rain clouds and splash, but a main effect in ASCAT appears sub-cell wind variability on the ocean surface due to convective downbursts. This variability makes the radar ocean returns more isotropic and prone to MLE flagging. Imprints of wind downburst on the ocean surface are typically larger than any rain (splash) imprints and therefore difficult to validate by RR. Buoy wind and rain validation has been carried out.

The buoy analysis reveals inaccuracies and systematic effects in ECMWF vector winds rather than in ASCAT winds under rainy conditions. However, the collocated buoy dataset is rather limited. Further analysis on the ASCAT wind speed and direction artifacts will be carried out provided that a larger buoy dataset becomes available. In addition, other independent data sources will also be explored, such as geostationary satellite RR product movies, drifter wind data, and vessels of opportunity (VOS) wind data.

The SA method is tested for a heavy rain case. The ASCAT singularity map identifies the main streamlines of the air flow. The presence of heavy rain induces clear singu-

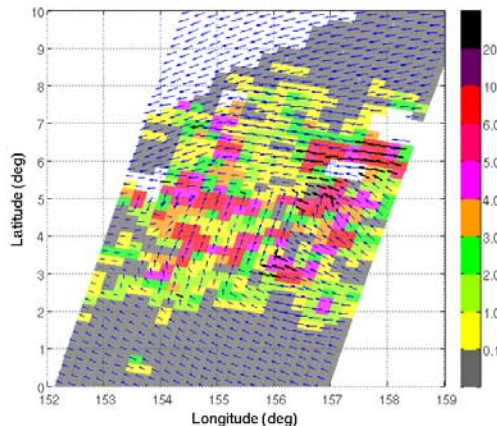


Fig. 3. Map of collocated ASCAT-TMI data acquired at 22:45 October 14, 2008. The coloured areas correspond to different TMI rain rates (see legend); blue arrows correspond to QC-accepted WVCs and bold black arrows to QC-rejected WVCs.

larity fronts, probably related to convective downbursts. Although separating rain-induced singularity fronts from wind-induced ones is challenging, preliminary results show the technique's potential to reveal characteristics of the scatterometer retrieved wind fields. To contribute to the current ASCAT operational retrieval and QC, further analysis is required. Besides the retrieved wind vector fields, other ASCAT-derived parameters, such as the backscatter measurements, the inversion residuals (MLE), and the retrieved wind components (i.e., U, V, speed and direction), can be used to generate singularity maps. These will reveal further characteristics of the ASCAT data and retrievals in convective areas, in order to better understand and improve the latter.

Both the MLE QC-based and the singularity analysis methods are expected to be more effective when applied on higher-resolution ASCAT products, i.e., 12.5-km and coastal products (see <http://www.knmi.nl/scatterometer/>). On the one hand, ASCAT is expected to better resolve higher resolution wind phenomena (e.g., convergence and downbursts); on the other hand, the rain splashing signal, being patchy and intermittent, is expected to become more evident at smaller ASCAT footprints. As such, we proceed to extend this study to the ASCAT high-resolution products.

5. REFERENCES

[1] Figa-Saldana, J., J.J.W. Wilson, E. Attema, R. Gelsthorpe, M.R. Drinkwater, and A. Stoffelen, "The advanced scatterometer (ASCAT) on Metop: a follow-on for European scatterometers," *Can. Jour. of Rem. Sens.*, vol. 28, no. 3, 2002.

[2] Van De Hulst, H.C., *Light Scattering by small particles*, John Wiley and Sons, New York, pp. 428, 1957.

[3] Boukabara, S.A., R.N. Hoffman, and C. Grassotti, *Atmospheric Compensation and Heavy Rain Detection for SeaWinds Using*

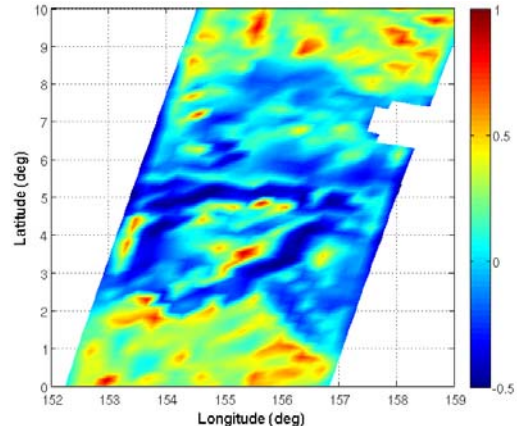


Fig. 4. Singularity map of the ASCAT retrieved wind field shown in Fig. 3. The map is constructed as the minimum exponents of the singularity maps associated to the U and V wind components.

AMSR, Atmospheric Environmental Research Inc., 131 Hartwell Ave., Lexington, Massachusetts (USA), 2000.

[4] Figa, J., and A. Stoffelen, "On the assimilation of Ku-band scatterometer winds for weather analysis and forecasting," *IEEE Trans. on Geoscience and Rem. Sens.*, vol. 38 (4), pp. 1893-1902, 2000.

[5] Nie, C. and D.G. Long, "A C-Band scatterometer simultaneous wind/rain retrieval method," *IEEE Trans. on Geoscience and Rem. Sens.*, vol. 46, no. 11, pp. 3618-3632, 2008.

[6] Stiles, B.W., and S. Dunbar, "A Neural Network Technique for Improving the Accuracy of Scatterometer Winds in Rainy Conditions," *IEEE Trans. on Geoscience and Rem. Sens.*, vol. 48, no. 8, pp 3114-3122, 2010.

[7] Stoffelen, A., and D. Anderson, "Scatterometer data interpretation: measurement space and inversion," *J. Atmos. and Oceanic Technol.*, vol. 14(6), 1298-1313, 1997.

[8] Hersbach, H., A. Stoffelen, and S. de Haan, "The improved C-band ocean geophysical model function: CMOD-5," *J. Geophys. Res.*, 112, C03006, doi:10.1029/2006JC003743, 2007.

[9] Portabella, M., and A. Stoffelen, "Rain detection and quality control of SeaWinds," *J. Atm. and Ocean Techn.*, vol. 18, no. 7, pp. 1171-1183, 2001.

[10] Portabella, M., A. Stoffelen, A. Verhoef, and J. Verspeek, "A new method for improving scatterometer wind quality control," *IEEE Geosci. Rem. Sens. Lett.*, in press 2012.

[11] Turiel A., J. Sole, V. Nieves, J. Ballabrera-Poy, and E. Garcia-Ladona, "Tracking oceanic currents by singularity analysis of Micro-Wave Sea Surface Temperature images," *Remote Sensing of Environment*, vol. 112, pp. 2246-2260, 2008.

[12] Isern-Fontanet, J., A. Turiel, E. Garcia-Ladona, and J. Font, "Microcanonical multifractal formalism: application to the estimation of ocean surface velocities," *J. Geophys. Res.*, 112:C05024, 2007.